arXiv:0810.2322v3 [physics.atom-ph] 26 Jan 2009

Hard x-ray attosecond Compton streak camera and SPIDER

G. L. Yudin,[1, 2, *] D. I. Bondar,[2, 3] S. Patchkovskii,[2] P. B. Corkum,[2, 4] and A. D. Bandrauk[1]
[1] *Université de Sherbrooke, Sherbrooke, Québec J1K 2R1, Canada*
[2] *National Research Council of Canada, Ottawa, Ontario K1A 0R6, Canada*
[3] *University of Waterloo, Waterloo, Ontario N2L 3G1, Canada*
[4] *University of Ottawa, Ottawa, Ontario K1N 6N5, Canada*

(Dated: January 26, 2009)

We formulate an analytic, semi-relativistic theory of an attosecond *Compton* streak camera and SPIDER (spectral phase interferometry for direct electric-field reconstruction) – proposing two new methods of measuring the duration of an hard x-ray pulse without fundamental restrictions on the measurement accuracy. Our approach is based on the generalization of the Furry picture and the theory of monochromatic photon scattering by a bound electron in the presence of a strong laser field. The resulting scheme has a simple structure and leads to a closed-form expression for the Compton ionization amplitude. We investigate Compton electron interference in the separable Coulomb-Volkov continuum with both Coulomb and laser fields treated non-perturbatively. Using a hydrogen atom as an example, we focus on the energy-resolved spectra of Compton electrons and methods for complete characterization of attosecond hard x-ray pulses.

PACS numbers: 32.90.+a, 34.10.+x, 34.90.+q

Introduction. —Attosecond science began in the 21st century starting with the experiment [1] where a train of 250-attosecond radiation pulses was obtained, and the measurement [2] which indicated a soft-x-ray pulse duration of 650±150 attoseconds (asec). Fundamental to the process, the generated attosecond pulses are synchronized with the infrared field. This very precise synchronization between the attosecond pulse and an intense laser field is prominent in attosecond science because the infrared field can provide the nonlinearity needed for attosecond measurement of attosecond pulses [3, 4, 5] of attosecond phenomena in physics, chemistry, and technology, see, e.g., Refs. [6, 7].

Recent developments in ultrafast hard x-ray sources [8] demonstrate that it is technically feasible to generate x-ray *attosecond pulses in Ångström wavelength range* [9, 10, 11] with free electron lasers (FELs). At the very heart of these proposals is the temporal synchronization scheme between FEL and an external laser, the so-called seeded attosecond x-ray radiation [10]. It is important to consider how the attosecond streak camera and SPIDER can be generalized to the hard x-ray range where there will be unexplored physical phenomena with dynamic response on the attosecond time scale.

We analyze one such process – Compton ionization. The relative contributions of photo- and Compton ionization are sensitive to the incident photon energy $\hbar\Omega$ and ionization potential I_p. In the case of a weakly bound electron ($I_p \ll \hbar\Omega$), Compton ionization prevails at (see, e.g., Ref. [12])

$$\hbar\Omega \gtrsim 3(Z_a)^{8/7} keV, \tag{1}$$

where Z_a denotes the exponential coefficient in the initial electronic wavefunction[1] $|i\rangle \propto \exp(-Z_a r)$. Therefore, Compton probe spectroscopy becomes feasible for hard x-rays where photoionization becomes less important. Transferring the ideas of the attosecond streak camera and SPIDER to laser-assisted Compton ionization is not trivial. The photon is scattered, not absorbed, by the weakly bound electron. Theoretical descriptions of the Compton ionization are also quite distinct from photoionization (see diagrams in Fig. 1). However, in spite of the differences we will show that the Compton electron contains all phase information on the incident pulse provided we select the momentum of the scattered photon.

Starting with an *ab initio* method, we develop a theoretical approach to describe laser-assisted attosecond Compton ionization. To obtain the appropriate semi-relativistic $\hat{S}^{(2)}$-matrix element, we include the separable Coulomb-Volkov continuum [13] into the Furry representation [14] and generalize the theory [15] of monochromatic photon scattering by a bound electron (more details are presented in Fig. 1 and explained below). Next, we analyze the attosecond *Compton* streak camera and SPIDER. We show that Compton electrons spectra depend on the phase of the laser field relative to the hard x-ray attosecond pulse, just as in the usual soft x-ray case [3, 4, 5]. Thus, from the spectrum of Compton electrons the relative phase of all frequency components of the attosecond pulse can be determined. Combined with its spectrum, which can be measured conventionally, the pulse is fully characterized.

Theory. —As it is well known from traditional quantum electrodynamics, a general solution of Maxwell equa-

---

*Electronic address: gennady.yudin@nrc.ca

[1] Unless stated otherwise, the Hartree atomic units ($|e| = m_e = \hbar = 1$ and the velocity of light $c \approx$137.036) are used below.

tion can be represented in the form of a superposition of plane waves. If electromagnetic field is confined to a cubic box of volume V, the photon momentum $\mathbf{k}$ can have only discrete values, $k_n \sim nV^{-1/3}$ $(n = 0, \pm 1, \pm 2, ...)$. The set k_n approaches a continuum when $V \to \infty$; thus, the sum over k_n transforms into a four-dimensional Fourier integral. To describe the *attosecond* incident photon field, we employ the following general representation:

$$\hat{\mathbf{A}}_1(\mathbf{r},t) = \mathbf{e}_1 \int d^3q \int_{-\infty}^{\infty} d\omega \frac{Q(\mathbf{q},\omega)}{\sqrt{\Omega_1'}} \hat{C}_{\mathbf{k}_1'\Omega_1'} e^{i\mathbf{k}_1'\mathbf{r} - i\Omega_1' t}, \tag{2}$$

where $\mathbf{e}_1$ is the polarization vector, $\mathbf{k}_1'$ and Ω_1' are momenta and energies of the incoming photons, $\Omega_1' = \Omega_1 + \omega$, Ω_1 is the central frequency, $\mathbf{k}_1' = \mathbf{k}_1 + \mathbf{q}$, $k_1' = \Omega_1'/c$, and $\hat{C}_{\mathbf{k}_1'\Omega_1'}$ is the photon annihilation operator.

Now we define the generally unknown function $Q(\mathbf{q},\omega)$. We confine ourselves to the experimental setup where the direction of the momentum $\mathbf{k}_1'$ is fixed. In this geometry, Eq. (2) contains only one-dimensional integral over q. Integration in the $S_{fi}^{(2)}$-matrix leads to δ-functions, one of which fixes the parameter ω. Having fixed ω, we also set the momentum $\mathbf{k}_1'$, i.e., remove the integral over q. Now we select the initial x-ray pulse as a sum of linearly chirped Gaussians with a characteristic temporal duration τ (cf. with the case of attosecond photoionization [13]),

$$\hat{\mathbf{A}}_1(\mathbf{r},t) = \mathbf{e}_1 Dc\sqrt{V} \int_{-\infty}^{\infty} \frac{R(\omega)}{\sqrt{\Omega_1'}} \hat{C}_{\mathbf{k}_1'\Omega_1'} e^{i\mathbf{k}_1'\mathbf{r} - i\Omega_1' t} d\omega, \tag{3}$$

where the general attosecond interference factor $R(\omega)$ is determined by the replica weights ζ_k as

$$R(\omega) = e^{-(1-i\xi)\omega^2\tau^2/2} \sum_k \zeta_k e^{i\omega t_k}, \tag{4}$$

where t_k is time of the replica maxima, $D = V^{-1}A_0\tau\sqrt{1-i\xi}$, A_0 is the amplitude of the pulse, and ξ is the dimensionless chirp. Eqs. (3) and (4) describe a set of attosecond pulses with the bandwidth invariant to the dimensionless chirp ξ. The individual pulse duration is $\tau_{FWHM} = 2\tau\sqrt{\ln 2}\sqrt{1+\xi^2}$.

Without loss of generality, we can fix the momentum of the final photon (the direction and frequency), so the scattered photon field is presented by a single plane wave,

$$\hat{\mathbf{A}}_2(\mathbf{r},t) = \mathbf{e}_2 c\sqrt{\frac{2\pi}{V\Omega_2}} \hat{C}^{\dagger}_{\mathbf{k}_2\Omega_2} e^{i\mathbf{k}_2\mathbf{r} - i\Omega_2 t}, \tag{5}$$

where $\mathbf{k}_2$ and Ω_2 are the momentum and energy of the outgoing photon, $k_2 = \Omega_2/c$ and $\hat{C}^{\dagger}_{\mathbf{k}_2\Omega_2}$ is the creation operator.

Treating the IR laser field classically in the dipole approximation, we define its vector potential as

$$\mathbf{A}_L(t) = -\frac{c}{\omega_0}\Big[\mathbf{E}_1 \sin(\omega_0 t) + \mathbf{E}_2 \cos(\omega_0 t)\Big] e^{-\delta|t|}, \tag{6}$$

where ω_0 is the laser field frequency, the electrical field component $\mathbf{E}_1$ is along the Cartesian z axis, while the vector $\mathbf{E}_2$ is along the x axis. The vector potential $\mathbf{A}_L(t)$ and electric field $\mathbf{E}_L(t) = -(1/c)d\mathbf{A}_L(t)/dt$ are turned on adiabatically at $t \to -\infty$ and turned off at $t \to \infty$ (i.e., $\delta \to +0$).

We will further consider semi-relativistic Compton ionization. A closed-form expression is available for the transition matrix element, provided that weakly bound electrons, $I_p/\Omega_1' \ll 1$, semi-relativistic photon energies, $\Omega_1'/c^2 \ll 1$, and $Z_a/c \ll 1$ are assumed. Following the approach originally developed for laser-free monochromatic x-ray scattering [16], one can obtain a first-order approximation for the $S_{fi}^{(2)}$-matrix. In the absence of the IR field, at the non-relativistic photon energies

$$S_{fi}^{(2)} = -(2\pi)^{5/2} iDR(\omega)\mathfrak{M}_{fi}(\mathbf{p}), \tag{7}$$

$$\mathfrak{M}_{fi}(\mathbf{p}) \approx (\mathbf{e}_1 \cdot \mathbf{e}_2) \frac{\langle f|\exp\left[i(\mathbf{k}_1' - \mathbf{k}_2)\mathbf{r}\right]|i\rangle}{\sqrt{\Omega_1'\Omega_2}}, \tag{8}$$

$$\omega \equiv \omega_1 = p^2/2 + I_p + \Omega_2 - \Omega_1, \tag{9}$$

where $\mathbf{p}$ is the asymptotic value of Compton electron momentum at infinity.

The six-fold differential probability of laser-assisted Compton ionization is then given by

$$\frac{d^6 P_{Comp}}{dp dO_e d\Omega_2 dO_2} \equiv S^{(6)}_{Comp} = \frac{(2\pi p\Omega_2)^2}{c^3} |\mathfrak{M}_{Comp}(\mathbf{p})|^2, \tag{10}$$

where $dO_e = \sin\theta_e d\theta_e d\varphi_e$ and $dO_2 = \sin\theta_2 d\theta_2 d\varphi_2$ are the elements of solid angles containing vectors $\mathbf{p}$ and $\mathbf{k}_2$. We can express the amplitude $\mathfrak{M}_{Comp}(\mathbf{p})$ in terms of the IR-field-free amplitudes as:

$$\begin{aligned} \mathfrak{M}_{Comp}(\mathbf{p}) &= D \sum_{m,n=-\infty}^{\infty} R(\omega)\mathfrak{M}_{fi}(\mathbf{p})(-1)^m i^n \\ &\times \; e^{-in\varphi_0} J_m(\mathscr{M}_1 - \mathscr{M}_2) J_n(\mathscr{N}), \end{aligned} \tag{11}$$

$$\omega \equiv \omega_2 = \omega_1 + [2(\mathscr{M}_1 + \mathscr{M}_2 + m) + n]\omega_0. \tag{12}$$

The argument of Bessel functions $J_m(x)$ in Eq. (11) depends on $\mathscr{M}_{1,2} = E^2_{1,2}/(2\omega_0)^3$. In the geometry, where two parameters $\mathscr{N}_{1,2} = \mathbf{p} \cdot \mathbf{E}_{1,2}/\omega_0^2$ are not zero simultaneously, the angle φ_0 is defined by the equations $\cos\varphi_0 = \mathscr{N}_1/\mathscr{N}$ and $\sin\varphi_0 = -\mathscr{N}_2/\mathscr{N}$, where $\mathscr{N} = \sqrt{\mathscr{N}_1^2 + \mathscr{N}_2^2}$; at $\mathscr{N}_{1,2} \to 0$ the sum over n in (11) tends to unity.

Applications. —There are many possibilities for measurement because Compton spectra depend on the laser polarization and Compton scattering geometry. We illustrate the general result (10)-(12) in the case of a linearly polarized laser field: $\mathbf{E}_L = \mathbf{E}_1$ and $\mathbf{E}_2 = 0$ in Eq. (6); the laser wavelength is 800 nm. It should be pointed out that in the hard x-ray scattering regime, due to approximate momentum conservation $\mathbf{p} \approx \mathbf{k}_1' - \mathbf{k}_2$, and outgoing continuum electron will preferably appear along $\mathbf{k}_1' - \mathbf{k}_2$. Accordingly, we choose the incoming x-ray polarization along the Cartesian z axis and use the scattering geometry where $\theta_e = 0$ and $\theta_2 = \theta = \pi$.

We consider Compton ionization by an isolated attosecond x-ray pulse and by two replicas of the same pulse; the central frequency of incident photon is Ω_1=8 keV. The hydrogenic $1s$ state is chosen as the initial electronic bound state. Assuming that the incoming photon is unpolarized, we average the probability of Compton ionization over its polarization and sum the probability over polarizations of the outgoing photon, i.e., the term $(\mathbf{e}_1 \cdot \mathbf{e}_2)^2$ in Eq. (8) is to be substituted by $(1+\cos^2\theta)/2$.

In Figs. 2 and 3 we report the energy-resolved spectra of Compton electrons at the laser field intensity $I = 2 \times 10^{12}$ W/cm^2. The scattered photon energy is fixed, Ω_2=7757 eV. This energy has been chosen in accordance with the value of hydrogen ionization potential and the Compton's formulas [17]

$$\Omega_2 = \Omega_1/(1+\mu) \approx (1-\mu)\Omega_1, \quad E_e \approx \mu(1-\mu)\Omega_1, \tag{13}$$

where $\mu = (\Omega_1/c^2)(1-\cos\theta)$.

As in the photoelectron streak camera, the strong laser field distorts the Compton electron spectrum on a subcycle time scale. Fig. 2 shows the Compton electron spectra which are produced by a single x-ray pulses of 100 asec FWHM and different chirps. Times of the pulse maxima are t_1=0 (curves marked by 1a, 1b, and 1c) and $t_1 = \pi/2\omega_0$ (curves marked by 2a, 2b, and 2bc). Appropriate chirps are: ξ=0 (curves 1a and 2a), ξ=3 (curves 1b and 2b), and ξ=-3 (curves 1c and 2bc). One can observe the distinct dependence of spectral maximum position and its amplitude on the t_1 and absolute value of the chirp. The maximum speed of streaking occurs at the time where $\mathbf{E}_1 \sin(\omega_0 t)$ is at an extremum. It is reflected in chirp sign dependence of the spectra: in the case of t_1=0, at different signs of the chirp, we can clearly see the difference between spectra (1b and 1c), while the spectra calculated at $t_1 = \pi/2\omega_0$ and $\xi = \pm 3$ are identical (curve 2bc).

The energy shift between electron wave packets, needed for a complete phase measurements, can be induced by laser-assisted Compton ionization. To demonstrate the Compton SPIDER, we show in Fig. 3 the electron spectra generated by two replicas of an attosecond pulse, each of 100 asec FWHM. Times of the pulse maxima are t_1=0 and $t_2 = \pi/2\omega_0$. Owing to time separation $\pi/2\omega_0$ between replicas, interference spectral fringes of periodicity $\approx 2\omega_0$ are observed. The periodicity depends slightly on the chirp and Compton electron energy, as is illustrated in the two insets. When the pulse is positively chirped, the fringes are observed to shift to lower energies on the low-energy side of the spectrum, and to higher energies on the high-energy side. To reconstruct the spectral phase from the Compton electron spectrum, one use the same algorithm as in photoelectron SPIDER [4, 5].

The practical requirements for measuring the momentum of the scattered photon are not severe. We estimate sensitivity of Compton electron spectra to the uncertainty $\delta\mathbf{k}$ in the measurement of the scattered photon momentum $\mathbf{k}_2$. In the most probable scattering geometry $\mathbf{p} \approx \mathbf{k}_1' - \mathbf{k}_2$. Then, broadening of the 1s Compton ionization spectrum is determined by the amplitude $\mathfrak{M}_{1s}$:

$$\mathfrak{M}_{1s} = \mathfrak{M}_{1s}^{(0)}(1+\Delta), \quad \Delta \sim \delta k/k_2, \tag{14}$$

where $\mathfrak{M}_{1s}^{(0)}$ is the Compton amplitude, calculated assuming an exact measurement of $\mathbf{k}_2$.

Conclusion. —We have developed a semi-relativistic analytical theory of the laser-assisted attosecond Compton ionization. Strong laser electric field acts as an ultrafast phase modulator for the Compton electron wavepackets. The theory is applicable for arbitrary laser-field polarizations and x-ray pulse parameters. If the x-ray pulse duration falls below one period of the laser field, two new methods for measuring hard x-ray pulse durations - attosecond Compton streak camera and SPIDER - are feasible. They require us to measure the scattered photon and electron in coincidence. If the scattered X-ray pulse is accurately measured, then similar to the photoelectron SPIDER, there are no fundamental limits to the resolution of attosecond Compton measurements.

Once the x-ray pulse(s) is characterized using a well understood atom such as hydrogen, a new frontier of attosecond science will be to utilize the Compton Streak Camera to measure unknown dynamics in target systems – nuclei, atoms, molecules or solids – just as the attosecond streak camera is used to measure dynamics initiated by attosecond XUV pulses or by recollision [6].

High-brilliance synchrotron radiation sources permit very high momentum resolution ($\sim$ 20 meV at 10 keV [18]) in Compton scattering experiments. This high precision in turn permits accurate measurements of the electron momentum density of atoms, molecules, and extended solids, stimulating developments of the theory of many-body systems [19]. Once attosecond x-ray pulses are produced and synchronized to other optical sources, they will become powerful tools to follow structure dynamics, each delay produces a single frame in an attosecond movie.

We appreciate the valuable discussion with A. A. Zholents. This work has been partially supported by NSERC Grant SRO 5796-299409/03.

[1] P. M. Paul *et al.*, Science **292**, 1689 (2001).
[2] M. Hentschel *et al.*, Nature **414**, 509 (2001).
[3] J. Itatani *et al.*, Phys. Rev. Lett. **88**, 173903 (2002); M. Kitzler *et al.*, Phys. Rev. Lett. **88**, 173904 (2002).

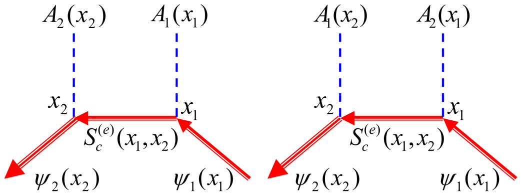

FIG. 1: (color online). Compton ionization diagrams included in our treatment. Notations 1 and 2 correspond to the initial and final electron and photon states. The four-vectors $x_{1,2} = (\mathbf{r}_{1,2}, it_{1,2})$. Dashed lines correspond to photon states, and solid lines describe electron states. $\psi_1(x_1)$ is the *laser-free* electron wavefunction, and $S_c^{(e)}(x_1, x_2)$ is the electron Green function. $\psi_2(x_2)$ is electron wavefunction in the separable Coulomb-Volkov continuum.

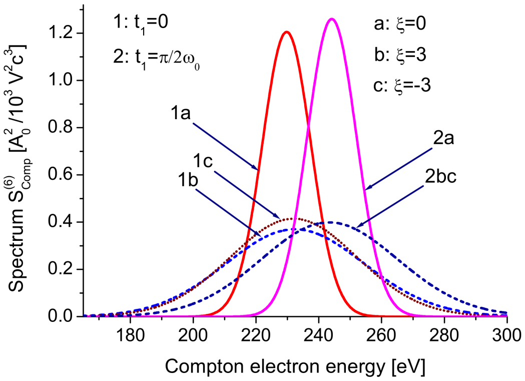

FIG. 2: (color online). Compton streak camera. Electron spectra are produced by a single x-ray pulses of 100 asec FWHM and different chirps. Times of the pulse maxima are t_1=0 (curves 1) and $t_1 = \pi/2\omega_0$ (curves 2). Other parameters are defined in the text.

[4] F. Quéré, J. Itatani, G. L. Yudin, and P. B. Corkum, Phys. Rev. Lett. **90**, 073902 (2003).

[5] J. Itatani, F. Quéré, G. L. Yudin, and P. B. Corkum, Laser Phys. **14**, 344 (2004).

[6] P. B. Corkum and F. Krausz, Nature Phys. **3**, 381 (2007).

[7] E. Goulielmakis *et al.*, Science **320**, 1614 (2008).

[8] J. Arthur *et al.*, Report SLAC-R-593, Stanford (2002) (see also http://www-ssrl.slac.stanford.edu/lcls/cdr/); M. Altarelli *et al.*, Preprint DESY 2006-097, DESY, Hamburg (2007) (see also http://xfel.desy.de).

[9] E. L. Saldin, E. A. Schneidmiller, and M. V. Yukov, Opt. Commun. **212**, 377 (2002); **237**, 153 (2004); **239**, 161 (2004); Phys. Rev. ST Accel. Beams **9**, 050702 (2006).

[10] A. A. Zholents and W. M. Fawley, Phys. Rev. Lett. **92**, 224801 (2004).

[11] A. A. Zholents, Phys. Rev. ST Accel. Beams **8**, 040701 (2005); A. A. Zholents and G. Penn, Phys. Rev. ST Accel. Beams **8**, 050704 (2005); A. A. Zholents and M. S. Zolotorev, New J. Phys. **10**, 025005 (2008).

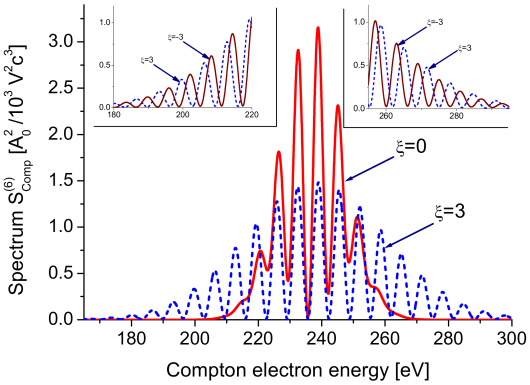

FIG. 3: (color online). Compton SPIDER. Electron spectra are generated by two replicas of an attosecond pulse of 100 asec FWHM. Times of two pulse maxima are t_1=0 and $t_2 = \pi/2\omega_0$. Chirp dependence is treated in the text.

[12] H. A. Bethe and E. E. Salpeter, *Quantum Mecanics of One- and Two-Electron Atoms* (Dover Publications, New York, 2008).

[13] G. L. Yudin, S. Patchkovskii, P. B. Corkum, and A. D. Bandrauk, J. Phys. B **40**, F93, 2223 (2007); G. L. Yudin, S. Patchkovskii, and A. D. Bandrauk, J. Phys. B **41**, 045602 (2008).

[14] W. H. Furry, Phys. Rev. **81**, 115 (1951).

[15] A. I. Akhiezer and V. B. Berestetskii, *Quantum Electrodynamics,* 3rd ed. (Nauka, Moscow, 1969).

[16] G. L. Yudin, Sov. Phys. Dokl. **21**, 591 (1976); A. M. Dykhne and G. L. Yudin, *Sudden Perturbations and Quantum Evolution* (Usp. Fiz. Nauk, Moscow, 1996).

[17] A. H. Compton, Phys. Rev. **21**, 207, 483 (1923).

[18] S. Huotari *et al.*, J. Synchrotron Rad. **12**, 467 (2005).

[19] I. G. Kaplan, B. Barbiellini, and A. Bansil, Phys. Rev. B **68**, 235104 (2003).